Preprint Title Characterization and Impact of Silver nanoparticles on cell growth, lipid, carbohydrate and fatty acids of *Chlorella vulgaris* and *Dictyochloropsis splendida*

Authors Sanaa M. M. Shanab, Abir M. Partila, Hamdy E. A. Ali and Mohd A. Abdullah

Publication Date 26 Aug 2019

Article Type Full Research Paper

ORCID® iDs Mohd A. Abdullah - https://orcid.org/0000-0001-8755-5444

Characterization and Impact of Silver nanoparticles on cell growth, lipid, carbohydrate and fatty acids of *Chlorella vulgaris* and *Dictyochloropsis splendida*

Sanaa Mahmoud Metwally Shanab[1], Abir M. Partila[2], Hamdy Elsayed Ahmed Ali[2], Mohd Azmuddin Abdullah[3,*]

[1]Department of Botany and Microbiology, Faculty of Science, Cairo University, 12613 Giza, Egypt

[2]Department of Radiation Microbiology, National Center for Radiation Research and Technology (NCRRT), Egyptian Atomic Energy Authority (EAEA), Egypt

[3]Institute of Marine Biotechnology, Universiti Malaysia Terengganu, 21030 Kuala Nerus, Terengganu, Malaysia

[*]Corresponding author: E-mail: azmuddin@umt.edu.my; joule1602@gmail.com

Tel: +609-668-3104; Fax: +609-668-3105

Abstract

Background: Many efforts have been made to increase the productivity of microalgae for biodiesel productions. The use of silver nanoparticles is the novel way to elicit stress responses with enhanced lipid level.

Results: In this study, the biosynthesis of extracellular silver nanoparticles (AgNPs) was reported and their impacts as elicitors on the cell growth and metabolite contents of *Chlorella vulgaris* and *Dictyochloropsis splendida* were evaluated. The production of AgNPs was achieved by the reduction of silver nitrate ($AgNO_3$) solution, after incubation at 35°C overnight with *Pseudomonas aeruginosa* supernatant, and exposed to gamma irradiation at 100 Gy for 1.5 mins.

The biosynthesis was confirmed by the maximum absorption peak at 455 nm with the UV–Vis Spectrophotometer. The Atomic Force Microscopy (AFM) recorded the spherical nanoparticles size of 10 nm, while the Dynamic Light Scattering (DLS) recorded the size range of 6.7 to 12.1 nm (84.2%) and the particles were monodispersed. The Gas Chromatography/Mass Spectroscopic analysis of the bacterial filtrate before reaction with $AgNO_3$ suggested the presence of ethylene glycol derivatives which may act as a reducing agent of silver ions to silver nanoparticles. Lower AgNPs concentrations (1, 3 and 5 mg/L) enhanced the lipid production but at the expense of cell growth. All AgNPs concentrations however displayed a negative impact on carbohydrates content. The lipid profile of the AgNPs-treated algae showed the appearance or disappearance, and increase or decrease of certain fatty acids, as compared to the

untreated control. The Saturated Fatty Acids represented the highest composition (61-67%) of the total fatty acids and Palmitic acids (16:0) were dominant (43.06-46.57%).

Conclusion: Lipids of this composition could withstand autoxidation during storage and are perfect feedstock for biodiesel and other lipid based applications.

Keywords: *Dictyochloropsis splendida*, *Chlorella vulgaris*, Cell growth kinetics, Lipid, Carbohydrate, Silver nanoparticles

1. Introduction

The field of nanotechnology has found diverse applications and the incorporation of nano-materials is increasing in a number of commercial products such as cosmetics, medicine, food packaging, odour-resistant textile, household applications and medical devices (as wound dressings) [1,2]. Metal nanoparticles have unique physico-chemical characteristics including catalytic and antimicrobial activities, and with their nano-size and highly precise surface area, the metal nanoparticles can easily penetrate the cell wall and interact with internal cellular biomolecules [3]. Silver, long known to exhibit inhibitory effects on microorganisms, is commonly present in medical and industrial process [4]. Silver nanoparticles (AgNPs) is one of the most widely synthesized particle which have effects on the growth of microorganisms, plants and mammalian cells[5-7]. The broad spectrum of antimicrobial properties of silver and AgNPs encourage its use in biomedical applications, water and air purification, food production, clothing, household products, cosmetics, contraceptives, cell phones, laptop keyboards, children's toys [8]. Nanoparticles such as AgNPs have exhibited different degrees of *in vitro* cytotoxicity [9,10].

Metal and metal oxide nanoparticles (such as Zn, Mg, Se, Cu, TiO_2, Fe_2O_3, MgO and Carbon) have been introduced as elicitors in different microalgal and cyanobacterial species. The use of trace or low nanoparticle concentrations has reportedly induced stimulation of algal biomass and pigment content with enhanced lipid production [11-16]. The effects of AgNPs on diatom *Skeletonema costatum* [17], *Thalassiosira pseudonana* and *Cyanobacterium synechococcus* sp. [18] and the eukaryotic green algae [6] have been reported. AgNPs have also been applied for cell wall disruption to release carbohydrate and lipid from *C. vulgaris* for biofuel production [19]. The AgNP-Algae interactions cause oxidative dissolution, reactive oxygen species (ROS) generation and synergistic toxic effects [20]. The nanoparticles may actually lead to excessive production of ROS resulting in oxidative stress, which

ultimately diverts the algal metabolic pathway away from the growth pathways into the production of hydrocarbon (lipids or carbohydrates) as storage compounds [16].

Synthesis of nanoparticles and nanomaterials are widely performed using physical, chemical or biological methods. The physical methods which include thermal decomposition, laser irradiation, condensation, diffusion, are low cost and environmentally-friendly, but has low yield. Chemical synthesis on the other hand may incorporate toxic chemical solvents and generate hazardous by-products [21]. Hence, the biological methods with microorganisms (bacteria, yeast, and fungi), algae or plants where the use of culture free-cells of these biological sources are considered as green chemistry approach, fast, and low cost but with high yield. These are widely utilized to reduce the chosen metal solution under controlled conditions and in most cases, the change in the color of the reaction solution is used as an indicator of the nanoparticle being synthesized [22]. The biosynthesis may occur intracellularly or the nanoparticles may be extracellularly released to the reaction solution from which the nanoparticles can be separated out by physical means [23]. The biosynthesis of metal nanoparticles may be triggered by several compounds present in the biological filtrate acting as reducing agents such as hydroxyl or carbonyl groups, terpenoids, phenolics, amines, proteins, pigments and alkaloids [24]. The biosynthesis of AgNPs, in certain conditions, is also attributed to the presence of enzyme Nitrate reductase [25].

The objectives of this study were to biosynthesize the AgNPs using bacterial filtrate of *Pseudomonas aeruginosa* strain (Accession no. 3NPO614) from Silver nitrate solution. The characteristics of the produced AgNPs were analysed by AFM and DLS. The effects of AgNPs on the cell growth, lipid, carbohydrate and free fatty acids content of the green microalgae, *Chlorella vulgaris* and *Dictyochloropsis splendida*, were investigated.

2. Materials and Methods

2.1. Bacterial strain cultivation and extracellular synthesis of AgNPs

The bacterial strain used for AgNPs biosynthesis was isolated from the soil sample contaminated with crude petroleum oil from Suez Canal, Egypt. The strain was molecularly identified (by 16S rRNA) as *Pseudomonas aeruginosa* and the sequence deposited in Genbank (Accession no. 3NPO 614).

The bacterial isolate was cultivated in LB broth (gL^{-1}): 10Tryptone, 5 yeast extract, 5 sodium chloride) [26] for 48 h at 37°C. After incubation, the cell-free supernatant was collected by centrifugation at 8000 rpm for 10 min in 250 ml conical flask. Solution of $AgNO_3$ (Sigma Chemical Co., USA) was added to the bacterial culture supernatant to get the final concentration of 3 mM $AgNO_3$, and the control was the culture supernatant only. The flasks were left over night at room temperature (35 C°), and then exposed to gamma irradiation of 100 Gy (Co-60 unit, 4000-A-India). for 1.5 mins at the National Center for Radiation Research and Technology (NCRRT), Egyptian Atomic Energy Authority (EAEA), Egypt. The color change from pale yellow to brown was visually checked, which indicated the extracellular synthesis of AgNPs. To evaluate the effect of gamma radiation on AgNPs synthesis, 3 mM $AgNO_3$ was irradiated by 100 Gy separately.

2.2. Characterization of AgNPs

The synthesized AgNPs were confirmed by using UV–Vis spectrophotometer (T60, UK) by detecting their maximum absorbance.

The size and shape of AgNPs were analyzed by the Atomic Force Microscopy (AFM) (Agilent 5500 AFM Scanning Probe Microscopy, USA). The microscopic images were recorded at different ranges of magnifications using silicon cantilever with force constant of 42 Nm^{-1}.

The size and dispersion of the AgNPs were characterized by the Dynamic Light Scattering (DLS, Zetasizer Nano ZS, UK). The size was determined using Nano ZS Zetasizer system (Malvern Instruments, UK). Before DLS measurement, the supernatant was passed through a 0.2 µm polyvinylidene fluoride (PVDF) membrane, and the sample was loaded into quartz microcuvette. Five measurements were performed and the mean was recorded. The conditions set were: a laser wavelength of 633nm (He-Ne), a scattering angle of 173° (fixed – without changing possibility), a measurement temperature of 25°C, a medium viscosity of 0.8872 mpa.s, a medium refractive index of 1.330 and a material refractive index of 0.200.

2.3. Determination of the bioreductant in the bacterial filtrate

The bacterial filtrate before reaction with $AgNO_3$ was analyzed by the Gas Chromatography/Mass Spectrometry (GC/MS, Trace GC1310-ISQ Mass Spectrometer, Thermo Scientific, USA) with a direct capillary column TG–5MS (30 m x 0.25 mm x 0.25 µm film thickness). The column oven temperature was initially held at 50°C and then increased by 7°C/min to 230 °C hold for 2 min, and increased by 15°C /min to the final temperature 290°C and held for 2 min. The injector and MS transfer line temperatures were kept at 250, 270°C respectively; Helium was used as a carrier gas at a constant flow rate of 1 ml/min. The solvent delay was 3 min and diluted samples of 1 µl were injected automatically using Autosampler AS1300 coupled with GC in the split mode. EI mass spectra were collected at 70 eV ionization voltages over the range of m/z 45–650 in full scan mode. The ion source temperature was set at 200 °C. The components were identified by comparison of their retention times and mass spectra with those of WILEY 09 and NIST 11 mass spectral database.

2.4. Effects of AgNPs on microalgal cell growth, lipid and carbohydrates

Two fresh water microalgae, *Chlorella vulgaris* and *Dictyochloropsis splendida*, were cultivated in BG-11 medium [27], consisting of (gL^{-1}): 1.5 $NaNO_3$, 0.04 K_2HPO_4, 0.075 $MgSO_4 \cdot 7H_2O$, 0.036 $CaCl_2 \cdot 2H_2O$, 0.006 citric acid, 0.006 ferric ammonium citrate, 0.02 Na_2CO_3, 0.001 Na-EDTA, and 1 ml of trace metal solution per liter. The trace metal solution contained (g L^{-1}): 2.86 H_3BO_3, 1.81 $MnCl_2 \cdot 4H_2O$, 0.222 $ZnSO_4 \cdot 7H_2O$, 0.39 $Na_2MoO_4 \cdot 2H_2O$, 0.079 $CuSO_4 \cdot 5H_2O$, 0.0494 $Co(NO_3)_2 \cdot 6H2O$. The cultures were maintained and subcultured for 25 days in 500 mL Erlenmeyer flasks, under continuous illumination of 40 µ E m^{-2} s^{-1} at 25ºC.

The effects of AgNPs concentrations (1, 3, 5, 15, 25 and 50 mg L^{-1}) on microalgal cell growth, lipid and carbohydrate contents were studied in 500 mL Erlenmeyer flasks under the previously described growth conditions.

2.4.1. Determination of Cell growth and kinetics parameters

Three ml of culture was sampled at regular interval of 5 days in triplicates and the cell growth was determined spectrophotometrically by measuring the optical density (O.D.) at 680 nm. The cell dry weight (D.W.) was measured gravimetrically every 5 days during the period of cultivation where 20 mL of culture samples were filtered through

pre-weighed filter paper (0.45 μm) and washed with deionized water. The filtered cells were dried at 60°C in the oven until constant weight, cooled in a desiccator, and then weighed. The D.W. was expressed as gL^{-1}.

The maximum specific growth rate, μ_{max} (d^{-1}), was calculated as:

$$\mu_{max} = \frac{1}{t} * ln\frac{x_f}{x_0} \dots\dots\dots\dots (1)$$

where X_f and X_o are the biomass D.W. ($g\ L^{-1}$) at the end and beginning of a batch run respectively, and t is the duration of the run (day).

The biomass productivity (BP) ($mg\ L^{-1}d^{-1}$) and biomass yield (BY) were calculated as follows [28]:

$$BP = \frac{(X_f - X_0)}{(T_2 - T_1)} \dots\dots\dots\dots (2)$$

$$BY = (X_f - X_0) \dots\dots\dots\dots (3)$$

where T_1 and T_2 (day) represent the incubation period of an experiment at the initial time (day 0) and the final day of incubation, respectively.

2.4.2. Determination of Lipid content

Lipids were extracted by a mixture of chloroform:methanol:deionized water at 1:1:0.9 ratios on volumetric basis [29]where 5 ml chloroform, 10 ml methanol, and 4 ml of deionized water were initially added to 0.3 g of dried algal biomass. The mixture was then shaken for 10 min, before another 5 ml of chloroform and 5 ml of deionized water added, and shaken overnight. The mixture was filtered to remove the algal pellets. The filtrate was transferred to a separatory funnel to allow separation of the organic and aqueous layers. The chloroform layer was evaporated using a rotary evaporator (40-45°C) and the extracted lipid was weighed to give lipid content as the percentage of the cell D.W:

$$L = \frac{W_L}{W_B} * 100 \dots\dots\dots\dots (4)$$

Where L is the lipid content (%), W_L and W_B are the weights of the extracted lipids and the dry biomass, respectively. The lipid productivity (LP) was calculated as follows [30]:

$$LP = BP * L \dots\dots\dots\dots (5)$$

where LP is the lipid productivity (mg $L^{-1}d^{-1}$), BP (mg $L^{-1}d^{-1}$) and L (% D.W.) are biomass productivity and lipid content, respectively.

Lipid yield was calculated as follows [31]:

$$LY = BY * L \dots\dots\dots\dots (6)$$

where LY is lipid yield (mg L^{-1}), biomass yield, BY (mg L^{-1}), L (% dry weight) are biomass yield and lipid content, respectively.

2.4.3. Fatty acids analyses

Fatty acid methyl esters (FAMEs) of the total lipid were prepared by transesterification using 2% sulphuric acid in methanol [32]. The fatty acid analysis was performed by gas chromatography (Perkin Elmer Auto System XL) equipped with flame ionization detector and a DB-5 silica capillary column (60 m ×0.32mm i.d.). The oven temperature was maintained initially at 45°C and then programmed to 60°C at a rate of 1°C/min, before finally programmed from 60°C to 240°C at a rate of 3°C/min. Helium was used as the carrier gas at the flow rate of 1 ml min^{-1}. The injector and the detector temperatures were set at 230°C and 250°C, respectively.

2.4.4. Determination of Carbohydrates

The phenol-sulfuric acid technique was used for total carbohydrate concentration determination with glucose as the standard **[33].** Five ml aliquot were taken from the cultures and centrifuged at 1500 rpm for 10 min. The pellets were re-suspended in 1 mL of distilled water and 1 mL phenol solution (10% w/v) was added. After thorough mixing, 5 mL of concentrated H_2SO_4 was quickly added and thoroughly mixed. The mixture was left to stand for 10 min at room temperature and then centrifuged at 3000 rpm for 10 min. The absorbance of supernatant was recorded at 485 nm against a reagent blank. Carbohydrate concentrations were obtained from a calibration curve of glucose with concentrations from 10 to 150 µg mL^{-1}.

2.5. Statistical analysis

177 The statistical analyses were performed using Minitab software (V18, Minitab Inc., State College, PA, USA). All the
178 experiments were conducted in triplicate. One-way ANOVA was used to determine the significance of difference in
179 dependent variables, and Tukey's test at a reliability level of $p<0.05$ was used to identify the differences between each
180 level of treatment.

181 **3. Results and discussion**

182 **3.1. Biosynthesis and characterizations of AgNPs**

183 The AgNPs formation from silver nitrate solution incubated with *P. aeruginosa* supernatant overnight at 35°C was
184 indicated by the change of the reaction mixture color from yellow to brown (Fig. 1). The UV–Vis spectrometry showed
185 the maximum absorption of AgNPs at 455 nm (Fig. 2), which was consistent with the recorded range at 400-450 nm
186 of AgNPs synthesized from various bioreductant such as bacterial supernatant [34-36]; [19]; [10], fungal filtrates [37-
187 48] . The range of the AgNPs maximum absorbance may be due to the variations in the bioreductant used, the AgNPs
188 size and the reaction conditions.

189 Table 1 shows the size of AgNPs synthesized from irradiation of 100 Gy and supernatant of *P. aeruginosa*
190 irradiated by 100 Gy and Fig. 3a exhibits the AgNPs size distribution based on DLS analysis. The $AgNO_3$ solutions
191 singly irradiated by gamma rays at 100 Gy dose produced AgNPs of 29.39-70.89 nm in which 90.9% were in the 34-
192 52nm range (Table 1 and Fig.3 a). The exposure of the supernatant reaction mixture to the same dose of gamma rays
193 produced the AgNPs of 6-12 nm, with 84.2% in the 6.77-12.18 nm size range, 14.8% at 14.4-21.18 nm; and 1% in
194 25.37-39.40 nm range (Table 1 and Fig 3b). In comparison, the AgNPs sizes were 5-35 nm when *P. aeruginosa*
195 filtrate is mixed with $AgNO_3$ solution and incubated at 85°C, pH 7 and 30 mins [34]. This means that the combination
196 of biological method and the 100 Gy irradiation produced the AgNPs of smaller nanosize than those produced by
197 biological method alone. The AFM images suggested that the AgNPs were roughly spherical in shape with sizes
198 mostly of 6-12 nm, monodispersed and not aggregated (Fig. 4).

199

200 **3.2. Determination of reducing agent**

201 GC/MS analysis of the bacterial filtrate revealed the predominant presence of ethylene glycol derivatives (Table 2)
202 which may act as reducing agent and participate in the reduction of silver ions (Ag^+) to silver nanoparticles (Ag^0).

These results were in agreement and conformity with previous reports [49, 50]). Cubic silver nanoparticles has been reportedly synthesized by the reduction of $AgNO_3$ using ethylene glycol at 140 C° in the presence of polyvinylpyrrolidone (PVP) and HCl [51]. The morphology of the produced AgNPs is suggested to be strongly influenced by the reaction conditions (temperature, $AgNO_3$ concentration, molar ratio of the units of PVP and $AgNO_3$). Polyol (alcohol containing hydroxyl group) such as ethylene glycol could act both as solvent and reducing agent. Three different shapes of AgNPs have been synthesized using ethylene glycol as reducing agent [52].

3.3. Effects of AgNPs on microalgal cell growth

Studies on AgNPs have focused mainly on the synthesis, characteristics, antimicrobial activities and the applications in different fields, including the AgNPs toxicity to living organisms, and the inhibition on the aquatic and terrestrial environments. Table (3) and Fig. (5) show that the maximum specific growth rates, biomass productivity and biomass yield of both *C. vulgaris* and *D. splendida* progressively decreased with increased AgNPs concentrations, as compared to the control. These reductions with AgNPs concentrations were in agreement with the growth inhibition of *Parachlorella kessleri* (by 30 and 60%) when exposed to bio- or chemo-synthesized AgNPs [53]. The adverse effect of AgNPs on the filamentous green algae *Pithophora oedogonium* and *Chara vulgaris* is exhibited in the progressive depletion of chlorophyll content and the mitotic disturbance is associated with the morphological malformation [6]. A study on soil content exposed to AgNPs, bulk Ag or Ag^+ for 6 days under controlled culture conditions reveals a marked inhibition of photosynthesis and biomass with a significant increase in cell size and membrane permeability [54]. The autotrophic algae *Chlamydomonas reinhardtii* in the water bodies, which receive effluents contaminated with various nanoparticles, has been found to experience initial toxic effect leading to the damage of ATP and photosynthesis due to the oxidative stress induced as a result of exposure to AgNPs [55].

Various algal species such as *Dunaliella tertiolecta* and *Chlorella vulgaris* [56], *Thalassiosira pseudonana* and *Cryobacterium synechococcus* [18], *Euglena gracilis* [57], and *Pseudokirchveriella subcapitata* [58] have been treated with different concentrations of AgNPs. The uptake, translocation and accumulation of AgNPs in algal cells depend on the cellular structure, membrane permeability, and the size of the nanoparticles [57]. The smaller size and the larger surface area to volume enable AgNPs to pass through the pores of the cell wall and reach the plasma membrane [59]. AgNPs may enter the cell membrane [60] and get attached to the various cell organelles and enhance the reactive

oxygen species (ROS) which affect the biochemical reactions of the algal cells [61]. From adhesion to cell membrane, as alternative to permeability or ion transport properties, the AgNPs may disturb cellular phosphate management, followed by inhibition of DNA synthesis by breaking the hydrogen bonding, and induce ROS generation, denaturation of ribosomes, and inactivation of enzymes and proteins through bonding on the active sites [62- 64].

Algae however do have specific mechanisms to tolerate and reduce the toxic effects of AgNPs or nanoparticles in general. On the entry of nanoparticles, algae may release metal-chelators which repress the availability of metal ions secreted through AgNPs or increase its intake of metals [65]. It may secrete certain compounds to increase the nanoparticles flocculation and decrease its availability [66 - 67]. Algal cells may also release organic carbon compounds that inactivate AgNPs toxicity [64]. Algal defence system generates low molecular weight antioxidant substances and enhances the production of antioxidant enzymes to combat and scavenge the excess ROS generated. The enhancement of biotic generation of antioxidant enzymes has been reported in *Chattonella marina* as a defence mechanism against the adverse effect of AgNPs on PS II, which may involve inhibition of electron transport activity and alteration of oxygen evolution [65] ;[20] ;[17]. Silver ions and AgNPs have reportedly altered the cell division and gene expression (cdc2 gene) in onion (*Allium cepa*) [68]. The AgNPs, or silver ions foliar application to 4-week old cucumber (*Cucumis sativus*) plant, significantly alter the metabolite profile with the activation of antioxidant defence system, and consequently inhibits respiration, alters membrane properties and reduces inorganic nitrogen fixation [69].

3.4. Effects of AgNPs on lipids and carbohydrates

Table (3) and Fig. (6a) show that 5 mg L^{-1} of AgNPs in *C. vulgaris* promoted the lipid content was elevated to 14.3% while 1-5 mg L^{-1} of AgNPs in *D. splendida* had the lipid content remained high at 14%. Further increase in AgNPs level resulted in growth retardation and reduced lipid content comparable to control in both species. In general, *D. splendida* showed lower biomass growth and lipid productivity, yield and content than the *C. vulgaris*. This result suggests that the effects of AgNPs may be species dependent or may suggest *D. splendida* was more susceptible to the oxidative stress than *C. vulgaris*. Fig. (6b) illustrates that increased AgNPs concentrations induced a significant and progressive decrease in carbohydrate yield in *C. vulgaris* and *D. splendida*.

The addition of inert nanoparticles in algal cultures may cause a nitrogen starvation condition which enhances lipid content in the algal biomass [70]. Improved lipid production has also been reported in *C. vulgaris* treated with TiO_2 and MgO nanoparticles which is attributable to induced oxidative stress [13]; [12]. *C. vulgaris* has been cultivated in growth media containing different concentrations of metal nanoparticles (Cu, Zn, Mg, Pb) to induce firstly the metal resistance capacity, before being cultivated in second media containing the metal salts of the corresponding nanoparticles under the same controlled culture conditions. As a result, the growth rate, biomass, cellular pigments, protein, carbohydrates and lipid production have increased depending on salt concentration as compared to control and wild strain [16]. The concept of intermediary medium has been proposed where *Morinda elliptica* cell cultures are first acclimatized in a stressed condition with high sucrose medium, before being grown in a production medium, also at high sucrose level, and with the resulting high productivity [71, 72]. In a study on the effect of carbon, ferric oxide and magnesium oxide nanoparticles on the green alga *Scenedesmus obliquus*, it is suggested that the algal metabolism modifies its normal pathways towards, in most cases, lipid production [15]. AgNPs have the ability to break the cell wall of the *C. vulgaris* to release the biomolecules such as proteins and lipids to be used for biodiesel production [19].

3.5. Effects of AgNPs on fatty acid profile

Table (4) exhibits the lipid profile of *C. vulgaris* and *D. splendida* before and after AgNPs treatment. Both showed comparable lipid profiles with more or less similar modifications (presence or absence, increase or decrease in certain fatty acid contents). The lipid profile includes the short and long chain saturated fatty acids (C12:0-C24:0). Some fatty acids such as lauric, linolenic, behenic and lignoceric acids which were not recorded in the control algae, were present after the AgNPs treatment. Other fatty acids such as heptadecanoic and eicosadienoic acids were recorded in the control algae, but disappeared after AgNPs treatment. Fatty acids production such as pentadecanoic, linoleic and linolenic acids were elevated, while stearic, oleic and arachidic acids were reduced upon the AgNPs treatment as compared to the control. Generally, the sum of the saturated fatty acids (SFAs) was increased in *C. vulgaris* and *D. splendida* (61.47 and 67.27%, respectively) as compared to the controls (54.88 and 52.81%, respectively). The unsaturated fatty acids (UFAs) contents were decreased from 45.11 to 39% and from 47.18 to 32.73%, respectively, while the monounsaturated fatty acids (MUFAs) decreased from 30.99 to 14.33 % and 33.57 to 15.75 %, respectively.

Palmitic acid (16:0) at 43.06% and 46.57% represented the highest composition, respectively, and Linoleic acid was the second highest at 20.62% and 20.12 %, respectively, in the AgNPs-treated algae. The high composition of SFAs at 61.47% and 67.27% in *C. vulgaris* and *D. splendida*, respectively, after AgNPs treatment as compared to the UFAs, MUFAs and polyunsaturated fatty acids (PUFAs) suggest that the produced lipids tend to be more stable and not susceptible to autoxidation (peroxidation) during storage. These lipids are good feedstock for biodiesel production and can be used blended with petroleum oil for transportation and other applications. The lipid profile analyses confirmed that the introduction of nanoparticles and stresses alter the metabolism of many algal species towards hydrocarbon production (lipids and/or carbohydrates) as reported earlier [70] ;[13] ;[12]; [16];[15].

4. Conclusion

The biosynthesis of AgNPs was successfully achieved from $AgNO_3$ and supernatant of *P. aeruginosa* after exposure to 100 Gy irradiation as confirmed by the maximum absorbance at 455 mm in UV–Vis spectrophotometer. The shape of AgNPs was spherical with sizes of 6-12nm at 84.2% as determined by AFM and DLS techniques. The reducing agent in the bacterial filtrate that reduce Ag^+ to Ag^0 may be ethylene glycol derivatives. Low concentrations of AgNPs (1,3 and 5 mg/L) enhanced lipid production in *C. vulgaris* and *D. splendida* but at the expense of cell growth. However, all AgNPs concentrations reduced the carbohydrates content. The lipid profile of AgNPs-treated microalgae revealed the dominance of palmitic acid (16:0) as well as the saturated fatty acids, suggesting the suitability and excellent criteria as feedstocks for biodiesel production and other lipid applications.

Conflict of interest

The authors declare that they have no conflict of interest

References

1. Service, R. F. Nanotechnols calls rise for more research on toxicology of nanomaterials. *Science.2005, 310*, 1609.

2. Chaudhari, P. R.; Masurkar, S. A.; Shidore, V. B.; Kamble, S. P. Antimicrobial Activity of Extracellularly Synthesized Silver Nanoparticles using *Lactobacillus* Species Obtained from VIZYLAC Capsule. *J. Appl. Pharm. Sci.* 2012, *02(03)*, 25-29.

3. Sirajunnisa, A. R.; Surindhiran, D. Nanosilver fabrication mediated by exopolysaccharides from *Pseudomonas fluorescens*. *Am. J. Pharmtech. Res.*2014, 4, 727-742.

4. Jiang, W.; Mashayekhi, H.; Xing, B. Bacterial toxicity comparison between nano- and micro-scaled oxide particles. *Environ. Pollut.* 2009,*157(5)*, 1619-1625.

5. Lee, D.Y.; Fortin, C.; Campbell, P. G. Contrasting effects of chloride on the toxicity of silver to two green algae *Pseudokirchneriella subcapitata* and *Chlamydomonas reinhardtii*. *Aquat. Toxicol.* 2005,*75(2)*, 127-135.

6. Dash, A.; Singh, A. P.; Chaudhary, B. R.; Singh, S.K.; Dash, D. Effect of silver nanoparticles on growth of eukaryotic green algae. *Nano-micro Lett.* 2012,*4(3)*, 158-165.

7. Assawah, S.; El-Badry, A.; EL-Kassas, H.; Hegab, D.; Amer, D. Silver nanoparticles biosynthesized by two marine macroalgae *Corallina afficinalis* and *C. mediferranea* as a new remedy against human skin fungal pathogen.8th International conference, Faculty of Science, Kafrelsheek University, 3-4 October 2018.

8.Marambio-Jones, C.; Hoek, E. M. A review of the antibacterial effects of silver nanomaterials and potential implications for human health and the environment. *J. Nanopart. Res.*2010, 12(5), 1531-1551.

9. Wicki, A.; Witzigmann, D.; Balasubramanian, V.; Huwyler, J. Nanomedicine in cancer therapy: challenges, opportunities, and clinical applications. *J. Control Rel.* 2015, 200, 138-157.

10. Abdullah, M. A.; Hussein, H. A.; Mohammad, H.; Ghazaly, M. M.; Laith A. A. Different Formulations of Microalgal Crude Extracts and Silver Nanoparticles having Cytotoxic Effects on Breast Cancer Cells (Malaysian Patent pending – PI 2018703319). 2018.

11. Griffiths, M. J.; Harrison, S. T. L. Lipid productivity as a key characteristic for choosing algal species for biodiesel production. *J. Appl. Phycol.*2009, *2(5)*, 493-507.

12. Kang, N. K.; Lee, B.;Choi, G. G.; Moon, M.; Park, M.S.; Lim, J.; Yang, J. W. Enhancing lipid productivity of *Chlorella vulgaris* using oxidative stress by TiO_2 nanoparticles. *Korean J. Chem. Eng. 2014,31(5)*, 861-867.

13. Sarma, S. J.; Das, R. K.; Brar, S. K.; Le Bihan, Y.; Buelna, G.; Verma, M.; Soccol, C. R. Application of magnesium sulfate and its nanoparticles for enhanced lipid production by mixotrophic cultivation of algae using biodiesel waste. *Energ.*2014, 78, 16-22.

14. Padrova, K.; Lukavsky, J.; Nedbalova, L.; Cejkova, A.; Cajthaml, T.; Sigler, K.; Rezanka, T. Trace concentrations of iron nanoparticles cause overproduction of biomass and lipids during cultivation of cyanobacteria and microalgae. *J. Appl. Phycol.*2015, 27(4), 1443-1451.

15. He, M.;Yan, Y.;Pei, F.;Wu, M.; Gebreluel, T.; Zou, S.; Wang, C. Improvement on lipid production by *Scenedesmus obliquus* triggered by low dose exposure to nanoparticles. *Sci. Rep.* 2017,*7(1)*, 15526.

16. Sibi, G.; Kumar, D.A.; Gopal, T.; Marinath, K.; Banupria, S.; Chaitra, S. Metal nanoparticle triggered growth and lipid production in *Chlorella vulgaris*. *Int. J. Sc. Res. Environ. Sci. Toxicol.*2017, 2(1), 1-8.

17. Huang, J.; Cheng, J.; Yi, J. Impact of silver nanoparticles on marine diatom *Skeletonema costatum*. *J. Appl. Toxicol.* 2016, *36(10)*, 1343-1354.

18. Burchardt, A. D.; Carvalho, R. N.; Valente, A.; Nativo, P.; Gilliland, D.; Garcìa, C. P.; Lettieri, T. Effects of silver nanoparticles in diatom *Thalassiosira pseudonana* and *Cyanobacterium synechococcus* sp. *Environ. Sci. Technol.* 2012, 46(20), 11336-11344.

19. Sirajunnisa, A. R.; Duraiarasan, S.; Mani, V. Biosynthesis of silver nanoparticles and its application in cell wall disruption to release carbohydrate and lipid from *C. vulgaris* for biofuel production. *Biotechnol. Rep.*2016, 11, 70-76.

20. He, D.; Dorantes-Aranda, J. J.; Waite, T. D. Silver Nanoparticle Algae Interactions: Oxidative Dissolution, Reactive Oxygen Species Generation and Synergistic Toxic Effects. *Environ. Sci. Technol.* 2012,*46(16)*, 8731-8738.

21. Wang, J.; Zhang, X.; Chen, Y.; Sommerfeld, M.; Hu, Q. Toxicity assessment of manufactured nanomaterials using the unicellular green algae *Chlamydomonas reinhardtii. Chemosphere.*2007, 73(7), 1121-1128.

22. Anderson, R. A. Algal culturing techniques. 2005,Elsevier, Amsterdam.

23. Samantarai, S. K.; Achakzai, K. K. Strategic designing of the algal culture system to obtain valuable products. *Middle-East J. Sci. Res.*2014, 22(4), 575-580.

24. Asmathunisha, N.; Kathiresan, K. A review on biosynthesis of nanoparticles by marine organisms. *Colloids Surf B Biointerfaces.* 2013, *103*, 283-287.

25. Anthony, K. J. P.; Murugan, M.; Gurunathan, S. Biosynthesis of silver nanoparticles from the culture supernatant of *Bacillus marisflavi* and their potential antibacterial activity. *J. Ind. Eng. Chem.* 2014, *20*, 1505–1510.

26. Martin, P. A. W.; Lohr, J.R.; Dean, D.H. Transformation of *Bacillus thuringiensis* protoplasts by plasmid deoxyribonucleic acid. *J. Bacterial.*1981, 145, 980-983.

27. Stanier, R. Y.; Kunisawa, R.; Mandel, M.; Cohen-Bazire, G. Purification and properties of unicellular blue-green algae (order Chroococcales). *Bacteriol. Rev.* 1971 ,35(2),171.

28. Vidyashankar, S.; VenuGopal, K. S.; Swarnalatha, G. V.; Kavitha, M. D.; Chauhan, V. S.; Ravi, R.; Bansal, A. K.; Singh, R.; Pande, A.; Ravishankar, G. A.; Sarada, R. Characterization of fatty acids and hydrocarbons of *Chlorophycean* microalgae towards their use as biofuel source. *Biomass Bioenerg.* 2015, 77, 75-9.

29. Bligh, E. G. ; Dyer, W. J. A rapid method of total lipid extraction and purification. *Can. J. Biochem. Physiol.* 1959, *37(8)*, 911-917.

30. Hempel, N.; Petrick, I.; Behrendt, F. Biomass productivity and productivity of fatty acids and amino acids of microalgae strains as key characteristics of suitability for biodiesel production. *J. Appl. Phycol.* 2012, *24(6)*, 1407-1418.

31. Yang, F.; Long, L.; Sun, X.; Wu, H.; Li, T.; Xiang, W.Optimization of medium using response surface methodology for lipid production by *Scenedesmus* sp. *Mar. Drugs.*2014, 12(3), 1245-1257.

32. Christie, W. Preparation of ester derivatives of fatty acids for chromatographic analysis. In: Advances in Lipid Methodology - Two. Christie, W. (Ed.) Oily Press, Dundee, Scotland. 1993,pp. 69-111.

33. Liu, D.; Wong, P. T. S.; Dutka, B. J. Determination of carbohydrate in lake sediment by a modified phenol-sulfuric acid method. *Wat. Res.* 1973, 7(5), 741-746.

34. Abo-State, M. A. M.; Partila, A. M. Microbial Production of Silver Nanoparticles by *Pseudomonas aeruginosa* Cell Free Extract. *J. Eco. Heal. Environ.* 2015, *3(3)*, 91-98.

35. Abo-State, M. A. M.; Partila, A. M. The Bactericidal Activities of Silver Nanoparticles (AgNPs) Produced by Cell-Free Supernatant of *Pseudomonas aeruginosa* and Sterilization by the Effect of Radiation. *J. Eco. Heal. Env.* 2017,*4(2)*, 61-68.

36. Abo-State, M. A. M.; Partila, A. M. Production of silver nanoparticles (AgNPs) by certain bacterial strains and their characterization. *Nov Res Microb. J.* 2018,1(2), 19-32.

37. Roy, S.; Mukherjee, T.; Chakraborty, S.; Das, T. K. Biosynthesis, characterization and antifungal activity of silver nanoparticles synthesized by the fungus *Aspergillus foetidus* MTCC8876. Dig *J. Nanomater. Biostruct.*2013, *8(1)*, 197-205.

38. Birla, S. S.; Gaikwad, S. C.; Gade, A. K.; Rai, M. K. Rapid synthesis of silver nanoparticles from *Fusarium oxysporum* by optimizing physic-cultural conditions. *Sci. World J. 2013*, 1-12.

39. Kamil, D.; Prameeladevi, T.; Ganesh, S.; Prabhakaran, N.; Nareshkumar, R.; Thomas, S. P. Green synthesis of silver nanoparticles by entomopathogenic fungus *Beauveria bassiana* and their bioefficacy against mustard aphid (*Lipaphis erysimi* Kalt.). *Ind. J. Exp. Biol.* 2017, *55*, 555-561.

40. Mahdieh, M.; Zolanvari, A.; Azimee, A.S. Green biosynthesis of silver nanoparticles by *Spirulina platensis*. *Sci. Iran* 2012, 19(3), 926-929.

41. Patel, V.; Berthold, D.; Puranik, P.; Gantar, M. Screening of cyanobacteria and microalgae for their ability to synthesize silver nanoparticles with antibacterial activity. *Biotechnol. Rep.*2015, *5*, 112-119.

42. Salari, Z.; Danafar, F.; Dabaghi, S.; Ataei, S. A. Sustainable synthesis of silver nanoparticles using macroalgae *Spirogyra varians* and analysis of their antibacterial activity. *J. Saudi Chem. Soc.*2016, 20(4), 459-464.

43. Omar, H. N.; Bahabri, F. S.; El-Gendy, A. M. Biopotential application of synthesis nanoparticles as Antimicrobial agents by using *Laurencia papillosa. Int. J. Pharmacol.* 2017,*13*, 303-312.

44. Abdel-Raouf, N.; Hozayen, W. G. M.; El Neem, M. A. Potentiality of Silver Nanoparticles Prepared by *Ulvafasciata* as Anti-nephrotoxicity in Albino Rats, *Egypt. J. Bot* .2017,*57 (3)*, 479-494.

45. Amin, M.; Anwar, F.; Janjua; M. R. S. A.; Iqbal, M. A.; Rashid, U. Green synthesis of silver nanoparticles through reduction with *Solanum xanthocarpum* L. berry extract: characterization, antimicrobial and urease inhibitory activities against *Helicobacter pylori*. *Int. J. Mol. Sci.* 2012, *13(8)*, 9923-9941.

46. Logeswari, P.; Silambarasan, S.; Abraham, J. Synthesis of silver nanoparticles using plants extract and analysis of their antimicrobial property. *J. Saudi Chem. Soc.* 2015,19 (3), 311-317.

47. Tripathi, D. K.; Tripathi, A.; Singh, S.; Singh, Y.; Vishwakarma, K.; Yadav, G.; Dubey, N. K. Uptake, accumulation and toxicity of silver nanoparticle in autotrophic plants, and heterotrophic microbes: a concentric review. *Front Microbiol.* 2017 8(7), 16-1.

48. Dykman, L. A; Shchyogolev, S. Y. The effect of gold and silver nanoparticles on plant growth and development, In: Saylor, Y. ; Irby, V. (Eds.) Metal nanoparticles, Nova Science Publishers, Inc.,2018, pp. 263-300

49. Sun, Y.; Xia, Y. Shape controlled synthesis of gold and silver nanoparticles. *Science*. 2002,298(5601*)*, 2176-2179.

50. Sun, Y.; Yin, Y.; Mayers, B.; Herricks, T.; Xia, Y. Uniform silver nanowires synthesis by reduction $AgNO_3$ with ethylene glycol in the presence of seeds and polyvinyl pyrrolidone. *Chem. Mater*.2002, 14, 4736-4745.

51. Im, S. H.; Lee, Y. T.; Wiley, B.; Xia, Y. Large scale synthesis of silver nanocubes: the role of HCl in promoting cube perfection and nanodispersity. *Angew. Chem. Int. Ed.* 2005,*44*, 2154-2157.

52. Wiley, B. J.; Chen, Y.; McLellan, J. M.; Xiong, Y.; Li, Z. Y.; Ginger, D.; Xia, Y. Synthesis and optical properties of silver nanobars and nanorice. *Nano Lett.* 2007, 7(4), 1032-1036.

53. Marzikova, A.; Velgosova, O.; Kavulicova, J. Effect of chemically and biologically synthesized Ag nanoparticles on the algal growth inhibition. Recent Advances on Environment, Chemical & Engineering and Materials. *AIP Conf. Proc. 1918*, 020008 (2017); https://doi.org/10.1063/1.5018503.

54. Nam, S. H.; An, Y. J. A rapid screening method to assess soil algal toxicity: Non-destructive sampling of algal cells using culture medium extraction. *Appl. Soil Ecol.* 2017, 120, 143-152.

55. Pellai, S.; Behra, R.; Nestler, H.;Suter, M. J. F.; Sigg, L.; Schirmer, K. Linking toxicity and adaptive responses across the transcriptome, proteome, and phenotype of *Chlamydomonas reinhardtii* exposed to silver. *Proc. Natl. Acad. Sci. USA*, 2014,111(9), 3490-3495.

56. Oukarroum, A.; Bras, S., Perreault, F.; Popovic, R. Inhibitory effects of silver nanoparticles in two green algae, *Chlorella vulgaris* and *Dunaliella tertiolecta*. *Ecotoxicol. Environ. Saf.* 2012,*78*, 80-85.

57. Li, X.; Schirmer, K.; Bernard, L.; Sigg, L.; Pillai, S.; Behra, R. Silver nanoparticle toxicity and association with the alga *Euglena gracilis*. *Environ. Sci. Nano*.2015¸ 2(6), 594-602.

58.Luruelle, S.; Sørensen, S. N.; Cupi, D.; Engelbrekt, C.; Veinot, J.; Baun, A.Toxicity of silver nanoparticles to green algae–towards a biotic ligand understanding. 7th International Conference on the Environmental Effects of Nanoparticles and Nanomaterials. 2013.

59. Samberg, M. E.; Orndorff, P. E.; Monteiro-Riviere, N. A. Antibacterial efficacy of silver nanoparticles of different sizes, surface conditions and synthesis methods. *Nanotoxicol.* 2011,5(2), 244-253.

60. Mueller, N. C.; Nowack, B. Exposure modeling of engineered nanoparticles in the environment. *Environ. Sci. Technol.*2008, 42(12), 4447-4453.

61. Miao, A. J.; Luo, Z.; Chen, C.S.; Chin, W.C.; Santschi, P. H.; Quigg, A. Intracellular uptake: a possible mechanism for silver engineered nanoparticle toxicity to a freshwater alga *Ochromonasdanica*. *PLoS One 2010, 5(12)*, e15196.

62. Moreno-Garrido, I.; Pérez, S.; Blasco, J. Toxicity of silver and gold nanoparticles on marine microalgae. *Mar. Environ. Res.* 2015,111, 60-73.

63.Kwok, K. W.; Dong, W.; Marinakos, S.M.; Liu, J. Chilkoti, A.; Wiesner, M.R.; Hinton, D.E. Silver nanoparticle toxicity is related to coating materials and disruption of sodium concentration regulation. *Nanotoxicol.* 2016,*10* (9), 1306-1317.

64. Taylor, C.; Matzke, M.; Kroll, A.; Read, D.S.; Svendsen, C.; Crossley, A. Toxic interactions of different silver forms with freshwater green algae and cyanobacteria and their effects on mechanistic endpoints and the production of extracellular polymeric substances. *Environ. Sci. Nano.* 2016, 3(2), 396-408.

65. Navarro, E.; Piccapietra, F.; Wagner, B.; Marconi, F.; Kaegi, R.; Odzak, N.; Behra, R. Toxicity of silver nanoparticles to *Chlamydomona sreinhardtii*. *Environ. Sci. Technol.*2008, 42(23), 8959-8964.

66. Soldo, D.; Hari, R.; Sigg, L.; Behra, R. Tolerance of *Oocystis nephrocytioides* to copper: intracellular distribution and extracellular complexation of copper. *Aquat. Toxicol.*2005, 71(4), 307-317.

67. Miao, A. J.; Schwehr, K. A.; Xu, C.; Zhang, S. J.; Luo, Z.; Quigg, A.; Santschi, P. H. The algal toxicity of silver engineered nanoparticles and detoxification by exopolymeric substances. *Environ. Pollut.* 2009,157(11), 3034-3041.

68. Fouad, A.S.; Hafez, R.M. Effect of silver ions and silver nanoparticles on cell division of onion (*Alium cepa*) and expression of cdc2 gene. *Biol. Plantarum.* 2018, *62(1)*, 166-172.

69. Zhang, H.; Du, W.; Peralta-Videa, J. R.; Gardea-Torresdey, J. L.; White, J. C.; Keller, A. A.; Guo, H.; Ji, R.; Zhao, L. Metabolomics Reveals How Cucumber (*Cucumissativus*) Reprograms Metabolites to Cope with Silver Ions and Silver Nanoparticle-Induced Oxidative Stress. *Environ. Sci. Technol.* 2018, 52(14), 8016-8026.

70. Subhasha, N.; Rai, M. P.; Sharma, R. Effect of nitrogen on growth and lipid content of *Chlorella pyrenoidosa. Am. J. Biochem. Biotechnol.* 2011, 7(3), 124-129.

71. Chong, T. M.;Abdullah, M. A.; Nor'Aini, M. F.; Lai, O. M.; Lajis, N. H. Anthraquinone production, Hydrogen peroxide level and antioxidant vitamins in *Morinda elliptica* cell suspension cultures from intermediary and production medium strategies. *Plant Cell Report.* 2004,*22*, 951-958.

72. Abdullah, M. A.; Lajis, N. H.; Ali, A. M.; Marziah, M.; Sinskey, A. J.; Rha, C. K. Issues in Plant Cell Culture Engineering for enhancement of productivity. *J. Develop. Chem. Engin. Min. Proc*. 2005,*13(5/6)*, 573-587.

Table captions

Table 1: The size of AgNPs synthesized from irradiation of 100 Gy and supernatant of *P. aeruginosa* irradiated by 100 Gy

Table 2: Major compounds in the supernatant of *P. aeruginosa*

Table 3: Kinetics of cell growth and lipid of *C. vulgaris* and *D. splendida* (Results represent mean ±SD of three replicates; different small letters indicate significant difference ($p<0.05$))

Table 4: The fatty acids profiles of *C. vulgaris* and *D. splendida* cultured on media with and without AgNPs (5 mg/L) synthesized by *P. aeruginosa* supernatant

Figure captions

Fig. 1: Visual observation of the biosynthesis of silver nanoparticles by supernatant of *P. aeruginosa*. (a) Control supernatant without $AgNO_3$ (no color change). (b) Bacterial supernatant with $AgNO_3$ solution (color change from pale yellow to brown).

Fig. 2: The UV–Vis absorption spectrum of silver nanoparticles synthesized by supernatant of *P. aeruginosa* and irradiated by 100 Gy.

Fig. 3: Size distribution of AgNPs synthesized from (a) irradiation by 100 Gy, (b) supernatant of *P. aeruginosa* irradiated by 100 Gy

Fig. 4: AFM images of mono-disperse AgNPs synthesized by *P. aeruginosa* supernatant irradiated by 100 Gy on silicon substrate.

Fig. 5: Growth curves of (a) *C. vulgaris*, (b) *D. splendida*, under the influence of different AgNPs concentrations synthesized by *P. aeruginosa* supernatant irradiated by 100 Gy (Error bars represent ±SD of three replicates).

Fig. 6: a) Lipid contents, b) Carbohydrate contents, of *C. vulgaris* and *D. splendida* cultured at different treatment of AgNPs concentrations synthesized by *P. aeruginosa* supernatant irradiated by 100 Gy (Different small letters on the same bars indicate significant difference ($p<0.05$); error bars represent ±SD of three replicates).

Table 1: The size of AgNPs synthesized from irradiation of 100 Gy and supernatant of *P. aeruginosa* irradiated by 100 Gy

Irradiated by 100 Gy		Supernatant of *P. aeruginosa* irradiated by 100 Gy	
Size of AgNPs (nm)	Volume (%)	Size of AgNPs (nm)	Volume (%)
29.39	5.5	6.78	5.60
34.03	21.0	7.84	18.40
39.41	32.2	9.08	25.40
45.64	25.8	10.52	21.20
52.85	11.9	12.18	13.60
61.2	13.2	14.11	7.60
70.89	0.4	16.34	4.00
82.09	0.0	18.92	2.10
		21.91	1.10
		25.37	0.50
		29.39	0.30
		34.03	0.10
		39.41	0.10

Table 2: Major compounds in the supernatant of *P. aeruginosa*

Compound name	R.T.	Area (%)	Molecular Formula
Octaethylene glycol monododecyl ether	12.09 -18.77 22.53- 31.48 32.48- 34.18 34.41- 34.72	30.40	$C_{28}H_{58}O_9$
Heptaethylene glycol	22.53- 26.95	0.48	$C_{14}H_{30}O_8$

Table 3: Kinetics of cell growth and lipid of *C. vulgaris* and *D. splendida* (Results represent mean ±SD of three replicates; different small letters indicate significant difference ($p<0.05$))

Microalgal species	AgNPs (mg L^{-1})	Max specific growth rate, μ_{max} (d^{-1})	Biomass productivity, *BP* (g $L^{-1}d^{-1}$)	Biomass yield, *BY* (g L^{-1})	Lipid productivity, *LP* (g $L^{-1}d^{-1}$)	Lipid yield, *LY* (mg L^{-1})
C. vulgaris	0	0.137 ± 0.002^{a}	0.064 ± 0.003^{a}	1.58 ± 0.047^{a}	0.63 ± 0.026^{a}	156.90 ± 5.14^{a}
	1	0.132 ± 0.003^{a}	0.056 ± 0.001^{b}	1.38 ± 0.036^{b}	0.39 ± 0.029^{a}	97.81 ± 4.44^{b}
	3	0.121 ± 0.005^{b}	0.052 ± 0.001^{b}	1.28 ± 0.050^{b}	0.31 ± 0.008^{b}	77.70 ± 2.25^{c}
	5	0.111 ± 0.003^{c}	0.039 ± 0.003^{c}	1.11 ± 0.116^{c}	0.57 ± 0.061^{bc}	158.76 ± 15.51^{a}
	15	0.092 ± 0.003^{d}	0.031 ± 0.003^{d}	0.76 ± 0.033^{d}	0.27 ± 0.031^{cd}	66.55 ± 3.34^{cd}
	25	0.088 ± 0.005^{d}	0.021 ± 0.002^{e}	0.62 ± 0.018^{d}	0.19 ± 0.026^{de}	55.52 ± 1.19^{d}
	50	0.071 ± 0.003^{e}	0.016 ± 0.002^{e}	0.42 ± 0.022^{e}	0.11 ± 0.018^{e}	29.95 ± 3.34^{e}
D. splendida	0	0.121 ± 0.011^{a}	0.041 ± 0.002^{a}	1.05 ± 0.063^{a}	0.38 ± 0.016^{a}	98.71 ± 5.55^{b}
	1	0.112 ± 0.011^{ab}	0.031 ± 0.002^{b}	0.82 ± 0.030^{b}	0.43 ± 0.024^{ab}	111.20 ± 3.23^{a}
	3	0.110 ± 0.007^{ab}	0.029 ± 0.001^{bc}	0.69 ± 0.042^{c}	0.39 ± 0.019^{ab}	96.62 ± 6.60^{b}
	5	0.097 ± 0.006^{bc}	0.024 ± 0.003^{cd}	0.59 ± 0.035^{d}	0.34 ± 0.039^{b}	82.34 ± 5.57^{c}
	15	0.088 ± 0.001^{cd}	0.018 ± 0.003^{de}	0.52 ± 0.031^{de}	0.16 ± 0.026^{c}	46.61 ± 3.46^{d}
	25	0.074 ± 0.003^{d}	0.015 ± 0.002^{e}	0.42 ± 0.030^{ef}	0.13 ± 0.019^{c}	36.70 ± 3.23^{de}
	50	0.070 ± 0.004^{d}	0.014 ± 0.003^{e}	0.35 ± 0.026^{f}	0.11 ± 0.016^{c}	28.90 ± 2.23^{e}

Table 4: The fatty acids profiles of *C. vulgaris* and *D. splendida* cultured on media with and without AgNPs synthesized by *P. aeruginosa* supernatant

Type of fatty acids	Fatty acid (%)			
	C. vulgaris		*D. splendida*	
	Control	AgNPs (5 mg/L)	Control	Ag NPs (1 mg/L)
Lauric acid (C12:0)	-	1.12	-	1.30
Myristic acid (C14:0)	0.34	3.30	-	2.60
Pentadecanoic acid (C15:0)	5.53	9.40	5.99	12.47
Palmitic acid (C16:0)	44.51	43.06	40.36	46.57
Palmitoleic acid (C16:1)	8.71	9.10	3.83	8.15
Heptadecanoic acid (C17:0)	1.11	-	1.86	-
Stearic acid (C18:0)	1.75	0.50	2.00	0.54
Oleic acid (C18:1)	22.28	5.23	29.74	5.60
Linoleic acid (C18:2)	12.13	20.62	12.60	20.12
Linolenic acid (C18:3)	-	3.58	1.01	3.92
Arachidic acid (C20:0)	1.63	0.47	2.60	-
Eicosadienoic acid (C20:2)	1.99	-	-	-
Behenic acid (C22:0)	-	1.10	-	1.16
Lignoceric acid (C24:0)	-	2.52	-	2.63
Saturated fatty acid	54.88	61.47	52.81	67.27
Unsaturated fatty acid	45.11	39.00	47.18	32.73
Monounsaturated fatty acid	30.99	14.33	33.57	13.75
Polyunsaturated fatty acid	14.12	24.2	13.61	24.04

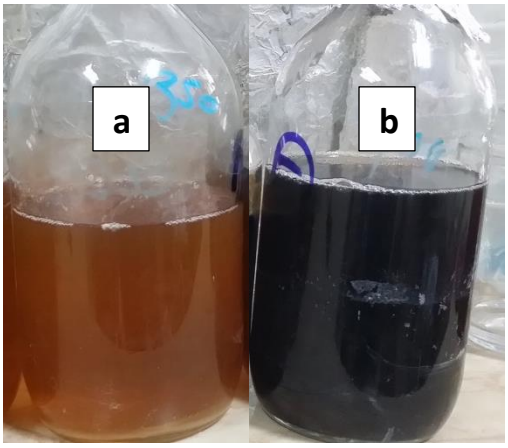

Fig. (1)

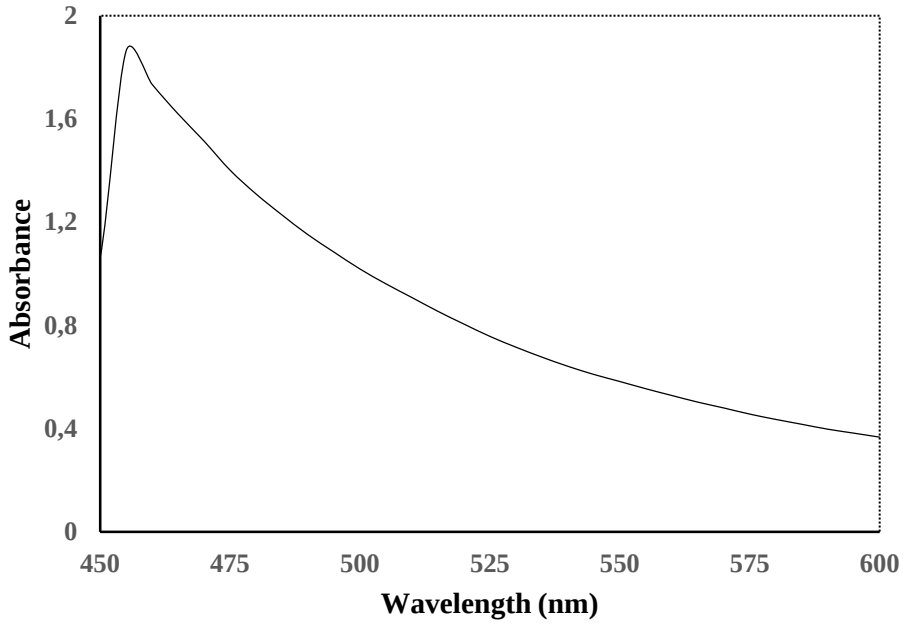
2
1,6
1,2
0,8
0,4
0
Absorbance
450
475
500
525
550
575
600
Wavelength (nm)

Fig. (2)

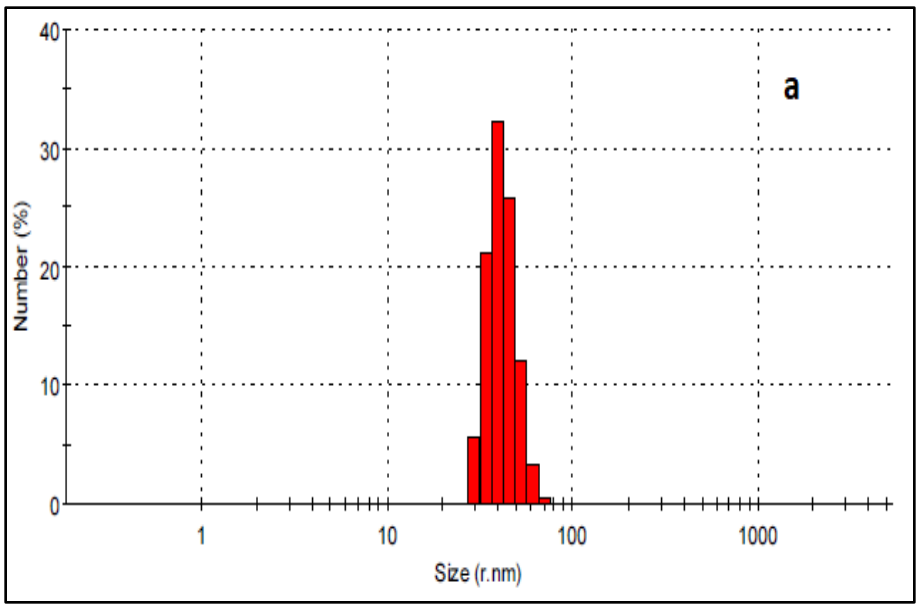
a
Number (%)
Size (r.nm)
0
10
20
30
40
1
10
100
1000

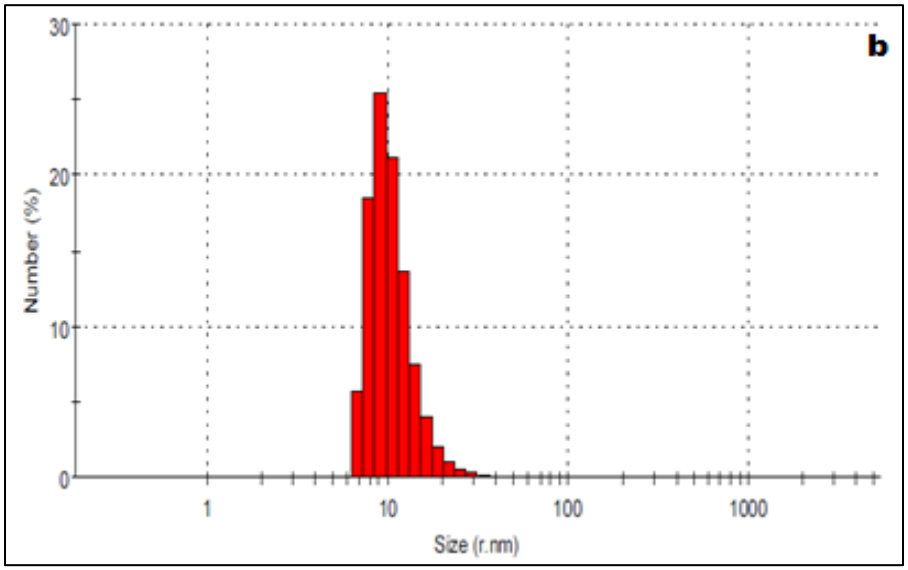
b
Number (%)
Size (r.nm)
0
10
20
30
1
10
100
1000

Fig. (3a, b)

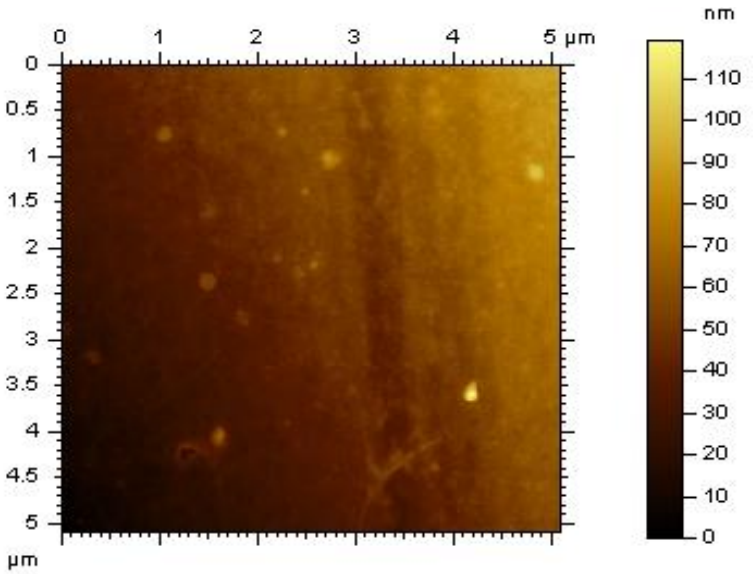
0
1
2
3
4
5 µm
0
0.5
1
1.5
2
2.5
3
3.5
4
4.5
5
µm
nm
110
100
90
80
70
60
50
40
30
20
10
0

Fig. (4)

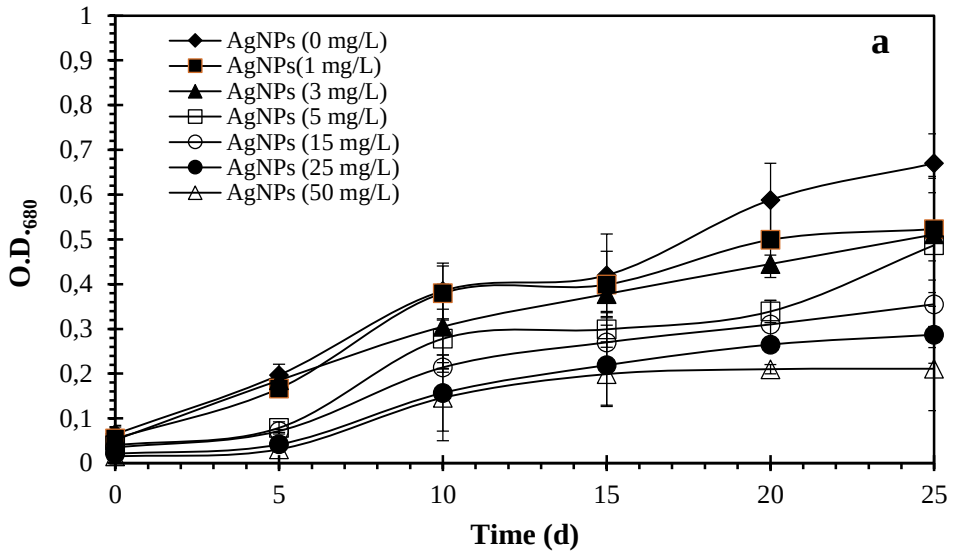

102

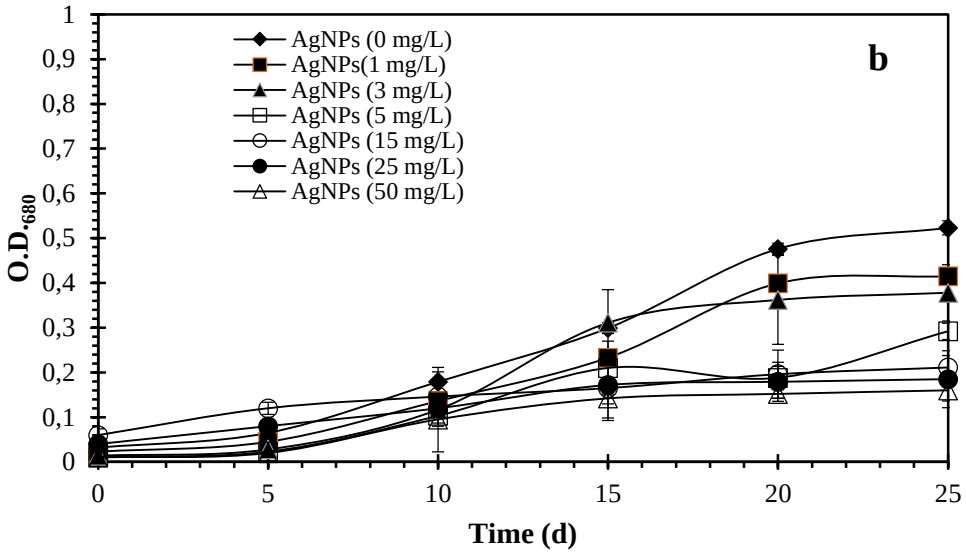

103

104

105 **Fig. (5 a, b)**

106

107

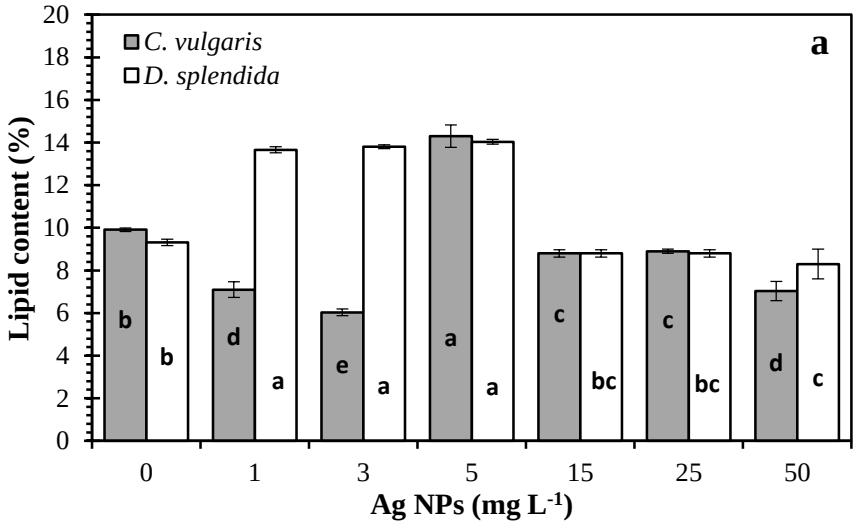
C. vulgaris
D. splendida
a
Lipid content (%)
Ag NPs (mg L-1)
0 1 3 5 15 25 50
b b d a e a a a c bc c bc d c

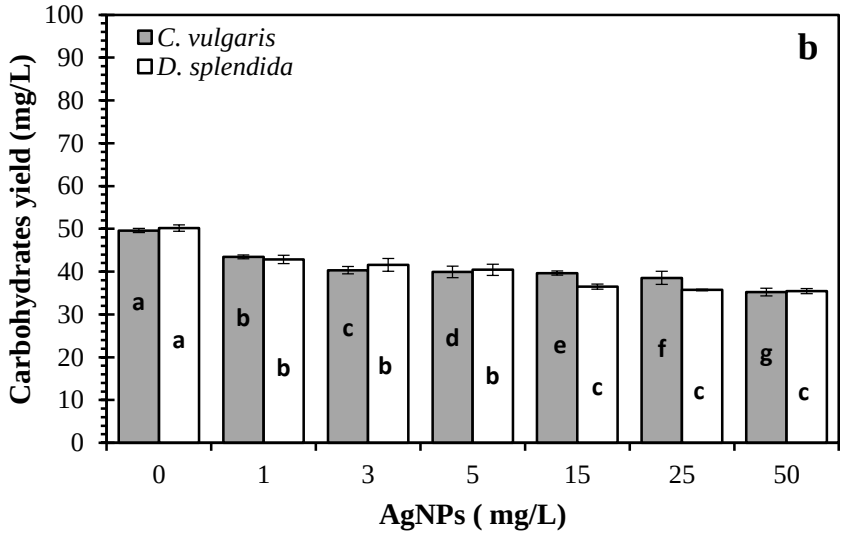
C. vulgaris
D. splendida
b
Carbohydrates yield (mg/L)
AgNPs (mg/L)
0 1 3 5 15 25 50
a a b b c b d b e c f c g c

Fig. (6 a, b)